An Integral Methodology for Predicting Long Term RTN

Kean H. Tok, Mehzabeen Mehedi, Jian F. Zhang, James Brown, Zengliang Ye, Zhigang Ji, Weidong Zhang, John S. Marsland, Asen Asenov, and Vihar Georgiev

***Abstract*—Random Telegraph Noise (RTN) adversely impacts circuit performance and this impact increases for smaller devices and lower operation voltage. To optimize circuit design, many efforts have been made to model RTN. RTN is highly stochastic, with significant device-to-device variations. Early works often characterize individual traps first and then group them together to extract their statistical distributions. This bottom-up approach suffers from limitations in the number of traps it is possible to measure, especially for the capture and emission time constants, calling the reliability of extracted distributions into question. Several compact models have been proposed, but their ability to predict long term RTN is not verified. Many early works measured RTN only for tens of seconds, although a longer time window increases RTN by capturing slower traps. The aim of this work is to propose an integral methodology for modelling RTN and, for the first time, to verify its capability of predicting the long term RTN. Instead of characterizing properties of individual traps/devices, the RTN of multiple devices were integrated to form one dataset for extracting their statistical properties. This allows using the concept of effective charged traps (ECT) and transforms the need for time constant distribution to obtaining the kinetics of ECT, making long term RTN prediction similar to predicting ageing. The proposed methodology opens the way for assessing RTN impact within a window of 10 years by efficiently evaluating the probability of a device parameter at a given level.**

***Index Terms*— Noise, Random telegraph noise (RTN), Jitters, Yield, Fluctuation, Device Variations, Time-dependent Variations.**

I. Introduction

Noise in MOSFETs adversely affects the performance of circuits [1-12]. IoT edge units are particularly vulnerable to it because the requirement of low power drives the operation voltage towards threshold level and reduces noise toleration [11],[12].

To optimize the circuit design, many efforts were made to model noise [1-12]. When devices are relatively large, there are many traps, and they collectively form 1/f noise. The impact of a single trap typically cannot be clearly observed and the modelling was mainly in the frequency domain [6]. As the device size shrinks to nano-meter scale, there are only a few traps in a device. The impact of a single trap increases and can be observed as Random Telegraph Noise (RTN) [1-12], where drain current exhibits step-like changes. The stochastic nature of trap distribution results in a large device-to-device variation (DDV) of RTN [1]-[5]. When compared with the time-independent DDV from other sources, such as discrete random dopants and line edge roughness [1], whose outliers can be screened out by pre-shipping tests of chips, the time-dependent DDV by RTN is difficult to screen out, as trapping may not occur within the limited test time window.

It has been reported that capturing one charge carrier by a trap can induce a shift of threshold voltage of tens of millivolts [3] and a fluctuation of current up to 10% [13]. This level of instability is comparable with that typically used to define the ageing-induced device lifetime [14]. They adversely impact circuit performance by causing, for example, jitters and malfunction of SRAM [4]. For future quantum computing at low temperature, this fluctuation can reach 50% [15].

To tackle these RTN-induced challenges, many recent efforts have been made to model RTN in the time domain [4],[5],[16]-[21]. To assess the impact of RTN on a circuit, a circuit designer needs the probability for device parameters at a given level within a time window. This can be accomplished through simulation, if one knows the number of traps in a device, their capture/emission times, and the shift induced by each trap [4],[5],[17]-[21].

To determine the statistical distributions of these parameters, a bottom-up approach was often followed: characterizing individual traps first and then grouping them together to fit an assumed cumulative distribution function (CDF) [3],[4],[19]-[21]. Most attentions have been paid to the CDF of RTN amplitude and the proposed CDFs include Exponential [3],[4],[10], Log-normal [4],[5],[8], and Generalized Extreme Value (GEV) [19]. These early efforts laid the foundation for current work.

For the average capture/emission times of a trap, the proposed CDFs include log-normal [9],[21] and log-uniform [5],[11],[22]. When compared with the amplitude, there is less data available on the capture /emission times [20],[21]. The number of capture/emission times obtained by the bottom-up approach is often less than 100 [20],[21], which is not large enough to reliably determine the CDFs. Without the CDFs of time constants, one could not predict RTN for different time windows. Some early works [13],[20] measured RTN with a time window of tens of seconds, whilst it is well known that RTN-induced fluctuation increases for longer time window. A number of compact models [16]-[18] were proposed by assuming that RTN magnitude and time constants follow

Manuscript received MM DD, YYYY. This work was supported by the Engineering and Physical Science Research Council of UK under the grant no. EP/T026022/1. The review of this paper was arranged by Editor XXX (Corresponding author: J. F. Zhang, e-mail: j.f.zhang@ljmu.ac.uk)

K. H. Tok, M. Mehedi, J. F. Zhang, J. Brown, Z. Ye, Z. Ji, W. Zhang, and J. S. Marsland are with School of Engineering, Liverpool John Moores University, Liverpool L3 3AF, UK. Z. Ji now is with School of Microelectronics, Shanghai Jiaotong University, Shanghai 200240, China.

A. Asenov and V. Georgiev is with the Department of Electronics and Electrical Engineering, University of Glasgow, Glasgow, G12 8QQ, U.K.

certain statistical distributions. It is not verified, however, that these models can be used to predict long term RTN.

The aim of this work is two-fold: to develop an integral methodology for extracting the CDF of RTN and, for the first time, to verify that the extracted model can predict long term RTN. This will be achieved through:

- Characterizing the impact of all traps on a device collectively, rather than individually. This removes the need of some early works of selecting devices with analyzable individual traps [13],[20];
- Integrating the RTN of multiple devices into one dataset to enable statistical analysis;
- Introducing the concept of "effective charged traps (ECT)", which removes the formidable burden of determining the capture and emission time constants of individual traps;
- Replacing the fixed number of traps per device, used by early works, with the time-dependent number of ECT. This mimics the modelling of ageing, where trap number increases with stress time through generation [14]. It transforms the distribution of time constants into the kinetics of ECT, simplifying the prediction of long term RTN;
- Introducing acceptor-like and donor-like traps to enable modeling both positive and negative parameter shift, which is widely observed experimentally but rarely modelled.

II. Integral Methodology

A. Raw data

Drain current, Id, was measured against time under a gate bias, Vg, of 0.5 V and drain bias, Vd, of 0.1 V, as reported in [11], and one example is given in Fig. 1(a). The Vg was chosen to be close to the threshold voltage, Vth, of 0.45 V for low power applications. The devices used are nMOSFETs with a channel length of 27 nm and channel width of 90 nm, fabricated by a 28 nm commercial CMOS technology. To catch fast traps, a sampling rate of 1 MSamples/sec was used and all tests were carried out at 125 ºC.

The reference Id, Iref, for each device was obtained from the average value of the first 10 measurement points. The relative shift of Id was evaluated from ΔId/Id=(Iref-Id)/Iref, so that a reduction of Id magnitude gives a positive ΔId/Id. The corresponding threshold voltage shift is estimated from ΔVth=ΔId/gm, where gm is transconductance and measured for each device from the slope of a pulse (3 μs) Id-Vg at Vg=0.5 V [23], which was taken before the RTN test. It should be pointed out that the error in ΔVth evaluated from ΔId/gm can be substantial if ΔId and gm were measured at Vg well above Vth [23]. In this work, they were measured at Vg=0.5 V, which is close to the Vth=0.45 V and the error is insignificant.

Based on the Id versus time measurement, early works [13],[20] often selected the devices that have analyzable RTN signals for extracting the amplitude and time constants of individual traps and discarded the devices where the fluctuation is too complex for such analysis. In this work, however, we focus on the collective impact of all traps on Id and do not decompose the Id fluctuation into contributions of individual traps experimentally. This removes the need for device selection and increases test efficiency.

The test in Fig. 1(a) was repeated on 402 devices and their ΔVth at a given time was integrated into one dataset for statistical analysis, as shown in Fig. 1(b). As time increases, the amplitude of fluctuation rises in Fig. 1(a), so that the |ΔVth| at a fixed CDF become larger in Fig. 1(b). Knowing this distribution will allow one to determine the probability of Vth at a specified level and in turn assess its impact on circuits. The challenge is how to model this distribution and how to predict it for longer times where test data are not available.

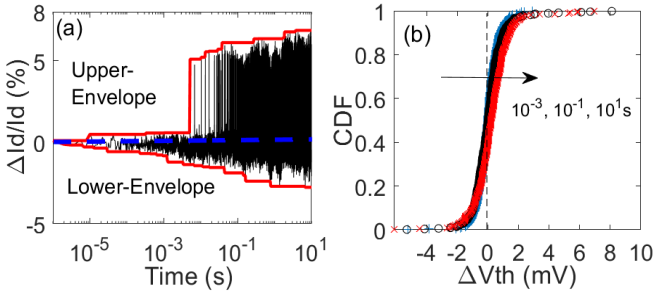

Fig. 1. (a) An example of measured data on one device, where ΔId>0 represents a reduction of Id from its reference value. The black lines are the ΔId/Id values, which can be either positive or negative. The red lines represent the upper and lower envelopes of the fluctuation. (b) The CDF of ΔVth=ΔId/gm at different time taken from 402 devices. For each device at a given time, the ΔId value was taken from a measurement like the one in (a). The distribution is not symmetric in ΔVth>0 and ΔVth<0.

B. The Concept of Effective Charged Traps (ECT)

The probability for a trap to be charged depends on the ratio of its average emission and capture time [2]. The statistical distribution of time constants is difficult to determine experimentally. To simplify tests, attempts were made to focus on either capture [11],[24] or emission [3].

Fig. 1(a) shows how to extract the envelope of the fluctuation, which is reached when multiple traps were simultaneously charged. Fig. 2 shows the average of the envelopes, which can be used to estimate the number of active traps for a given time window. As different devices hit their envelopes at different times, Fig. 2 shows that the average of measured ΔVth is substantially smaller than their average envelopes. In Section III.B, we will estimate the percentage of traps that are charged.

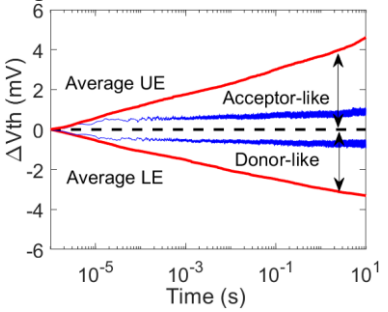

Fig. 2. A comparison of the average ΔVth>0 and ΔVth<0 of 402 devices (blue lines) with their average Upper and Lower envelopes (UE and LE). Using the envelopes will overestimate the impact of RTN.

The envelopes have been used to estimate the worst impact of RTN [11],[24],[25]. To optimize circuit design, however, one needs to model the probability of ΔVth at any level between

the two envelopes, which is the objective of this work.

To effectively take emission into account without evaluating the emission time of individual traps, we propose the concept of 'effective charged traps (ECT)'. The inspiration for this concept comes from the use of effective trap density for assessing the impact of ageing on devices [14],[26]. To evaluate trap density, one need knowing their spatial distribution in gate dielectric. This spatial distribution, however, is difficult to determine. To overcome this difficulty, one can assume all traps being at the interface so long as they produce the same ΔVth. The equivalent density of traps at the interface is referred to as effective trap density [26].

Similarly, to simulate the impact of RTN on devices and circuits, what is needed is the CDF in Fig. 1(b), rather than the detailed physical processes that this CDF originates from. For a given RTN-induced ΔVth at a time in Fig. 1(b), one can assume that it originates from a set of traps that are always charged. These 'effective charged traps (ECT)' ignore emission, but will produce the same CDF as, i.e. statistically equivalent to, that measured experimentally where emission occurs. By using the collective impact of a set of ECT to model CDF, as detailed in Section II.D, this integral approach does not require characterizing the capture and emission time of individual traps, greatly reducing modelling and testing time.

C. Acceptor-like and Donor-like Traps

Fig. 1(a) shows that ΔId=(Iref-Id) can be either positive or negative, resulting in the corresponding positive and negative ΔVth in Fig. 1(b). Early works [3],[4],[8],[10] typically only modelled ΔVth>0, since the popular Exponential and Log-normal distributions require ΔVth>0. Fig. 3 shows that the distribution of ΔVth in both ΔVth>0 and ΔVth<0 is considerable and there is little correlation between them, so that we must model the fluctuation in both directions, as we cannot infer one from the other.

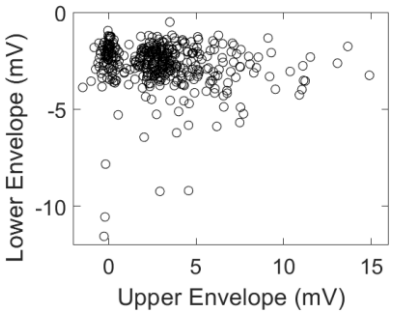

Fig. 3. The lower-envelope is plotted against the upper-envelope at 10 sec for 402 devices. There is little correlation between these two.

The shift in positive direction, i.e. ΔVth>0, for nMOSFETs is widely interpreted as traps capturing electrons from the conduction channel. Such traps can be either neutral or negatively charged and will be referred to as acceptor-like traps [26]. There can be different explanations for ΔVth<0. One of them is that some traps were pre-filled with electrons when Iref was measured. These pre-filled electrons could be emitted during measurement, resulting in ΔVth<0. Another is that there are donor-like traps, which can be either neutral or positive [26], and positive charges can result in ΔVth<0.

The measured data in this work cannot determine which explanation is correct and such determination is not required for achieving the aim of this work: proposing an integral method for predicting the long term RTN. For the convenience of presentation, we will use the acceptor-like traps for ΔVth>0 and donor-like traps for ΔVth<0, hereafter [26]. This allows ΔVth being modelled in both directions through,

$$\Delta Vth = \Delta Vth_A + \Delta Vth_D, \quad (1)$$

where $\Delta Vth_A>0$ and $\Delta Vth_D<0$ represent the contribution from acceptor-like and donor-like traps, respectively.

D. Modelling Procedure at a given time

To model the RTN-induced CDF in Fig. 1(b) by a set of ECTs at a given time, one needs to determine the number of traps per device, n, and the statistical distribution of threshold voltage shift caused by one trap, δVth. It should be noted that δVth is the shift per trap, which is different from the shift per device, ΔVth.

Statistically, it is well accepted that n follows a Poisson's distribution [4],[10]. The agreement on the distribution of δVth has not been reached and the popular assumptions include Exponential [3],[4],[10] and Log-normal [4],[5],[8]. In addition, Generalized Extreme Value (GEV) distribution has been proposed recently [19]. All three will be used in this work.

For a given δVth probability distribution function (pdf), the pdf of n_A number of acceptor-like traps can be evaluated from:

$$pdf_A(\Delta Vth_A) = Conv\left[pdf(\delta Vth_1), pdf(\delta Vth_2) \ldots pdf\left(\delta Vth_{n_A}\right)\right], \quad (2)$$

where ΔVth_A is the combined shift caused by n_A acceptor-like traps. When an analytic formula is not available, the Convolution (Conv) in Eq.(2) can be carried out numerically trap-by-trap: first between pdf(δVth_1) and pdf(δVth_2), the result is then convoluted with pdf(δVth_3). This continues until $\mathrm{pdf}(\delta \mathrm{Vth}_{n_A})$ is convoluted.

To overcome the difficulty that Exponential and Log-normal pdf requires δVth>0, we evaluate the magnitude of δVth for n_D donor-like traps by,

$$pdf_D(|\Delta Vth_D|) = Conv[pdf(|\delta Vth_1|), pdf(|\delta Vth_2|) \ldots pdf(|\delta Vth_{n_D}|)]. \quad (3)$$

The pdf[$\Delta Vth=\Delta Vth_A-|\Delta Vth_D|$] can be evaluated from:

$$pdf[\Delta Vth(n_A, n_D)] = \int_{-\infty}^{\infty} pdf_A[\Delta Vth(n_A, n_D) + x] pdf_D(x) dx. \quad (4)$$

The pdf[$\Delta Vth(n_A,n_D)$]) in eq.(4) is the probability for a device to have a ΔVth, if every device has n_A acceptor-like and n_D donor-like traps. After taking into account that both acceptor-like and donor-like traps follow Poisson distributions, the pdf(ΔVth) becomes:

$$pdf(\Delta Vth) = \sum_{n_A=0}^{\infty}\sum_{n_D=0}^{\infty} \frac{e^{N_A}N_A^{n_A}}{n_A!}\frac{e^{N_D}N_D^{n_D}}{n_D!} pdf[\Delta V_{th}(n_A, n_D)], \quad (5)$$

where N_A and N_D are the average number of effective acceptor-like and donor-like traps per device, respectively.

Finally, the measured ΔVth contains both RTN and thermal noise, which follows a Normal distribution. The thermal noise is taken into account by using:

$$pdf(\Delta Vth) = Conv[pdf(\Delta Vth_{RTN}), pdf(\Delta Vth_{Thermal})]. \quad (6)$$

III. Results and Discussions

A. Extracting model parameters

Based on the equations (1)-(6), the model parameters are extracted by the Maximum Likelihood Estimation (MLE) [19]. They include the statistical distribution parameters of δVth in Table I, the average number of acceptor-like and donor-like traps per device, N_A and N_D, and the standard deviation of thermal noise.

As an example, Fig. 4(a) shows that the fitted CDFs with test data at 10 sec by assuming Exponential, Log-normal and GEV distributions, respectively. To quantify the discrepancy between the data and the fitted CDF, Fig. 4(b) gives the sum of square error (SSE) per device. The SSE reduces in the order of Exponential, Log-normal, and GEV.

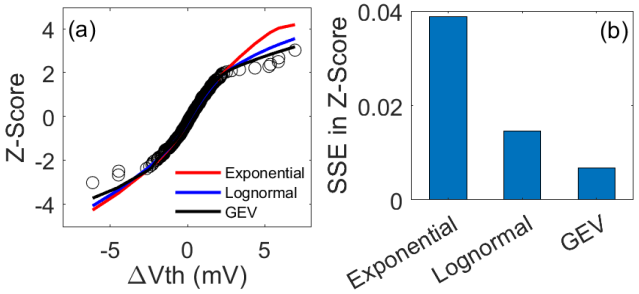

Fig. 4. (a) The CDF fitted based on the effective charged traps at 10 sec. The symbols are test data and the lines are fitted. (b) compares the sum of squared errors (SSE) per device for the three statistical distributions.

Table I. The pdf formula and their average parameter values extracted between 10^{-4} and 10 sec. The parameters η, α, β, and σ have the unit of mV.

	PDF of δVth	Acceptor	Donor
Exponential	$\frac{1}{\eta}e^{-\frac{\delta Vth}{\eta}}$	$\eta = 0.56$	$\eta = 0.48$
Lognormal	$\frac{1}{\delta Vth\theta\sqrt{2\pi}}e^{(-\frac{(\ln(\delta Vth)-\epsilon)^2}{2\theta^2})}$	$\epsilon = -0.43$ $\theta = 0.12$	$\epsilon = -0.71$ $\theta = 0.16$
GEV	$\frac{1}{\beta}(k)^{\xi+1}e^{-k}$ $k = \left(1+\xi\left(\frac{\delta Vth-\alpha}{\beta}\right)\right)^{-\frac{1}{\xi}}$	$\xi = 0.35$ $\alpha = 0.43$ $\beta = 0.34$	$\xi = 0.42$ $\alpha = 0.59$ $\beta = 0.19$
Thermal	$\frac{1}{\sigma\sqrt{2\pi}}e^{-\frac{1}{2}\left(\frac{\Delta Vth}{\sigma}\right)^2}$	$Exponential, \sigma = 0.11$ $Lognormal, \sigma = 0.13$ $GEV, \sigma = 0.13$	

Similar to Fig. 4 at 10 sec, the test data at other times are also fitted. Figs. 5(a) and 5(b) show the extracted average number of acceptor-like (N_A) and donor-like (N_D) traps per device against time, respectively. As expected, they increase with time, as longer time activates slower traps. There are more acceptor-like traps than donor-like traps, resulting from the skewed distribution towards positive ΔVth in Fig. 1(b). GEV gives the highest numbers, while Exponential has the lowest ones. At 10 sec, GEV has N_A =2.3 and N_D=2.

The extracted average δVth induced by one trap, μ, is given in Figs. 5(c) and 5(d) for acceptor-like and donor-like traps, respectively. In agreement with early work [20],[25], μ is independent of the time. The acceptor-like traps have larger μ than the donor-like traps. GEV gives the largest μ and Exponential gives the lowest. It should be noted that the average μ is in a range of 0.5 ~ 0.8 mV, indicating that there are small δVth that can be difficult to measure directly.

The other parameters for δVth distributions are insensitive to time, either, since δVth is the shift per trap. Their values are given in Table I.

B. Prediction of effective charged traps

Using the concept of ECT for modelling RTN converts the distribution of traps' time constants into a time dependent number of ECT, as shown in Figs. 5(a) and 5(b). This transforms the prediction of long term RTN to finding the kinetics of ECT, similar to predicting device ageing [14]. For ageing, power law is the well-known kinetics [14]. For the time constant distribution of RTN, two distributions were proposed: a uniform distribution against logarithmic time (Log-uniform) [5],[11] and a scaled Log-normal distribution [9],[21]. These three kinetics will be tested against the experimental data next.

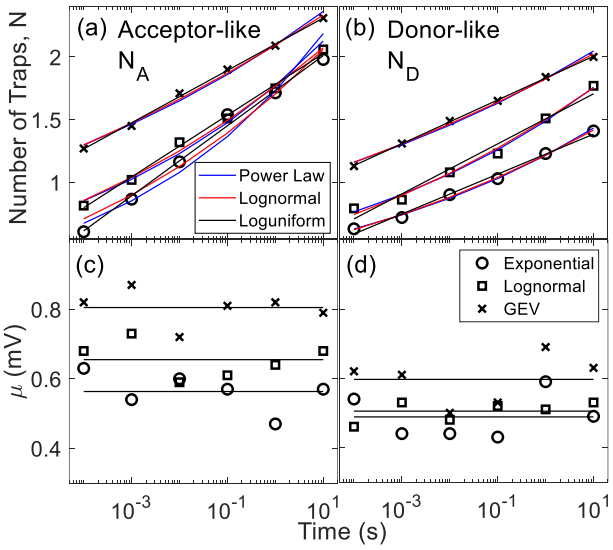

Fig. 5. The extracted average number of acceptor-like (a) and donor-like (b) traps per device at different time, based on different δVth distributions. The lines in (a) and (b) are the fitted kinetics. The extracted average δVth per trap, μ, is given in (c) for acceptor-like traps and in (d) for donor-like traps. The lines in (c) and (d) are the mean values.

All three kinetics can fit test data reasonably well over five orders of magnitude in time between 10^{-4} and 10 sec with the

relative Root-Mean-Square-Error (RSME) of a few percent. As a result, good fitting with test data is not sufficient to justify a model. If a model is correct, it should be able to not only fit test data, but also predict the long term RTN where test data is not used for fitting.

To further verify these kinetics, the RTN tests were extended from 10 to 6×10^4 sec. In Fig. 6, the symbols are extracted from test data. The data scattering beyond 10 sec is larger, since 402 devices were used between 10^{-4} and 10 sec and only 51 devices were used for the time-consuming tests of 6×10^4 sec.

The solid lines in Fig. 6 were the kinetics fitted with data between 10^{-4} and 10 sec and the data beyond 10 sec were not used for the fitting. These fitted kinetics were then extrapolated from 10 to 6×10^4 sec, as represented by the dashed lines. Although the differences between the fitted solid lines appear small, they become substantial for the extrapolated dashed lines as time increases. The sum of squared errors is summarized in Figs. 7(a) and 7(b) and discussed next.

For the Exponential δVth distribution, the Log-normal kinetics gives the lowest error for N_A in Figs. 6(a) and 7(a), but N_D agrees better with the power law, as shown in Fig. 6(d) and 7(b). It should be noted, however, even though the power law gives the lowest error for N_D with Exponential δVth, i.e. the first blue bar on the left in Fig. 7(b), this blue bar is higher than the errors of Lognormal and GEV δVth.

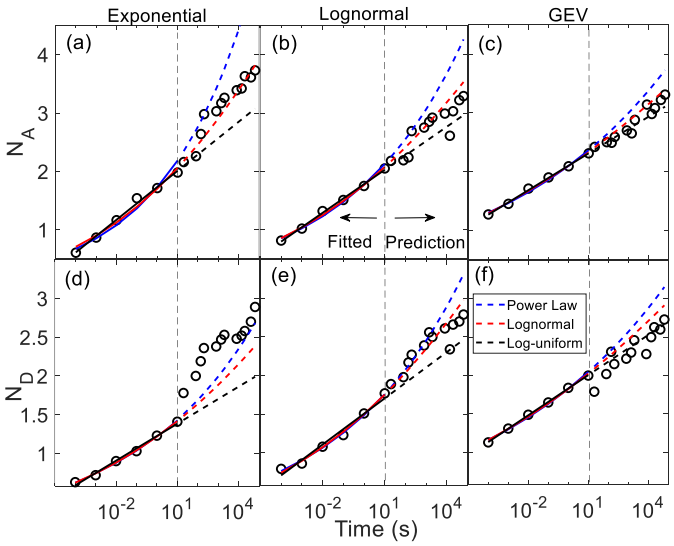

Fig. 6. Predicting the average number of acceptor-like traps, N_A, in the top row (a, b, c) and donor-like traps, N_D, in the bottom row (d, e, f). Symbols are extracted by fitting with the δVth distribution of Exponential in the left column (a, d), Log-normal in the middle column (b, e), and GEV in the right column (c, f). The solid lines were fitted with symbols between 10^{-4} and 10 sec for different kinetics. The dashed lines were extrapolated to 6×10^4 sec. The symbols beyond 10 sec were not used for fitting.

For N_A with Log-normal δVth distribution, Fig. 7(a) shows that power law has the highest error and errors are similar for Log-normal and Log-uniform kinetics. For N_D, Figs. 6(e) and 7(b) show that Log-normal kinetics has the lowest error. For GEV δVth distribution. Figs. 6(c), 6(f), 7(a) and 7(b) show that Log-uniform has the lowest error for both N_A and N_D.

The CDF of Log-normal kinetics should lead to an eventual saturation of N_A and N_D as time increases [11]. It, however, can fit the test data within the measurement window without approaching its saturation. As a result, we cannot rule it out based on current data.

Based on Figs. 6 and 7, the power law gives poor prediction of RTN overall. The RTN and ageing follows different kinetics, therefore. RTN interacts with device ageing. On one hand, the traps responsible for the RTN can also contribute to the charge build-up during ageing tests, such as bias temperature instability (BTI) [27],[28]. On the other hand, it has been reported that, after stress, some RTN signal can disappear for some time and then reappear [27]. One may speculate that stress releases some hydrogenous species, which interact with the RTN trap through temporary bonding, deactivates the RTN, and then migrate away [14],[27]. The detailed physical process is beyond the scope of this work.

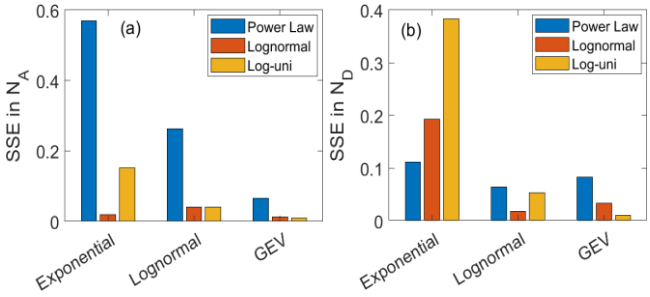

Fig. 7. The sum of squared errors for the prediction in Fig. 6 for acceptor-like (a) and donor-like (b) average number of traps per device. The lowest errors were obtained for Log-uniform kinetics with GEV δVth distribution.

We now estimate the percentage of ECTs against the active traps available for a given time window. The average number of active acceptor-like (N_{EA}) and donor-like (N_{ED}) traps per device can be estimated from the Upper- and Lower-Envelopes in Fig. 2 by dividing their average δVth per trap, i.e. μ, given in Figs. 5(c) and 5(d), respectively. Fig. 8 gives the ratio of ECT, i.e. N_A and N_D extracted for the GEV distribution in Figs. 6(c) and 6(f), against N_{EA} and N_{ED}, respectively. This ratio represents the average occupancy of traps. The time in Fig. 8 is the time window for measuring RTN. At short time window, over 50% traps are effectively charged. The occupancy decreases for longer time window and settles around 1/3. As longer time window allows capturing slower traps, this indicates that slower traps have lower occupancy than faster traps.

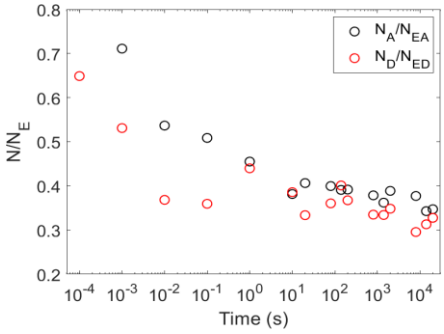

Fig. 8. The ratio of Effective Charged Traps, N_A and N_D, against the active traps available estimated from the Upper-envelope, N_{EA}, and Lower-Envelope, N_{ED}, respectively.

Figs. 2 and 6 show that the number of traps is time window dependent. In some early works, the number of traps in a device is specified without clearly giving a time window. In our opinion, this specification is incomplete. For example, when measured with a limited time window, a device may have zero trap. It, however, does not rule out that there are slower traps in this device. As a result, a time window should be given when specifying the number of traps in a device. If the time constant of traps follows a Log-uniform distribution, one cannot determine the total number of traps in a device in principle, although some devices can have a limited number of traps statistically.

C. The CDF Prediction of long-term RTN

As discussed in the introduction, the probability distribution function is what a designer needs for assessing the impact of RTN within a given time window. The question is how well one can predict the long-term CDF of RTN, based on the parameters extracted over a short time. For the first time, we attempt to predict the CDF of RTN at 6×10^4 sec by the model extracted from the data between 10^{-4} and 10 sec.

For each δVth distribution, the number of acceptor-like and donor-like traps at 6×10^4 sec is predicted by the kinetics of the lowest errors, as given in Table II. The statistical parameters of δVth distribution and thermal noise are assumed to be independent of time and their values given in Table I were used. With these parameters, the probability for one device to have a given ΔVth can be calculated directly, making the RTN simulation more efficient than the Monte Carlo simulation.

Figs. 9(a) and 9(b) compare the measured and predicted CDF at 6×10^4 sec for the Exponential, Log-normal and GEV δVth distributions. For the Exponential, the kinetics used is Log-normal for acceptor-like traps and power law for donor-like traps. For the Log-normal δVth distribution, Log-normal kinetics were used for both acceptor-like and donor-like traps. For the GEV, Log-uniform kinetics were used for both acceptor-like and donor-like traps. Fig. 9(c) shows that the errors reduce in the order of Exponential, Log-normal, and GEV. A reasonable agreement is obtained with test data, as shown in Figs. 9(a) and 9(b). This verifies the integral methodology proposed and its ability to predict the RTN at 6×10^4 sec based on data measured between 10^{-4} and 10 sec, a factor of 6×10^3 ahead. If one uses the data between 10^{-4} and 6×10^4 sec to make the prediction, it is reasonable to expect that one can predict a factor of 6×10^3 ahead, again. This will take the time to 3.6×10^8 sec, which is beyond 10 years.

Table II. The kinetics fitted with data between 10^{-4} and 10 sec.

δVth distribution	ECT	Kinetics
Exponential	N_A	$12.8 * \left[\frac{1}{2} erfc\left(-\frac{\ln(t)-21.5}{19.1\sqrt{2}}\right)\right]$
	N_D	$1.2152 * t^{0.0716}$
Lognormal	N_A	$13.1 * \left[\frac{1}{2} erfc\left(-\frac{\ln(t)-24.8}{22.5\sqrt{2}}\right)\right]$
	N_D	$13.3 * \left[\frac{1}{2} erfc\left(-\frac{\ln(t)-29.04}{24.2\sqrt{2}}\right)\right]$
GEV	N_A	$0.091 * \ln(t) + 2.1$
	N_D	$0.076 * \ln(t) + 1.83$

IV. CONCLUSIONS

The capability to predict the long term RTN by the models developed in early works has not been verified and this work proposes an integral methodology and verifies its capability to make this prediction. Instead of characterizing the contribution of individual traps to RTN, the impact of traps in a device was measured collectively and there is no need for selecting devices. Through integrating RTN measured on multiple devices into one dataset and using the concept of effective charged traps (ECT), the statistical distribution of device parameters at a given time is modelled, removing the formidable burden of characterizing the time constants of individual traps. This transforms the distribution of time constants to the kinetics of ECT, making the prediction of long term RTN similar to predicting ageing. The accuracy of RTN amplitude distribution per trap proposed by early works was assessed, including Exponential, Log-normal, and Generalized Extreme Value (GEV). The three kinetics examined are power law, Log-normal, and Log-uniform. The power law gives poor prediction and RTN follows different kinetics from ageing. Fluctuations in both positive and negative directions are modelled through using acceptor-like and donor-like traps. The work shows that this integral methodology can predict RTN by a factor of 6×10^3 ahead, opening the way for predicting RTN to 10 years based on measurements in a time window of one day.

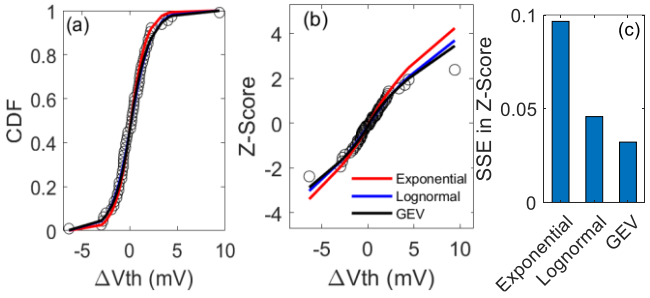

Fig. 9. Predicting the CDF of RTN at 6×10^4 sec based on the models extracted from the data between 10^{-4} and 10 sec. The symbols were measured data and the lines were the predicted CDF by using the N_A and N_D predicted in Fig. 6 and the average μ in Figs. 5(c) and 5(d). The CDF is plotted linearly in (a) and in Z-score in (b). The lines in (a) and (b) are the CDF fitted with different δVth distributions. (c) shows that the minimum error was obtained with GEV δVth distribution and Log-uniform kinetics.

ACKNOWLEDGMENT

The authors thank D. Vigar of Qualcomm Technologies International Ltd for supplying test samples and J. Franco of IMEC for useful discussions.

REFERENCES

[1]. A. Asenov, R. Balasubramaniam, A.R. Brown, J.H. Davies "RTS amplitudes in decananometer MOSFETs: A 3D simulation study," *IEEE Trans. Electron Devices*, vol. 50, no. 3, pp. 839-845, 2003, doi: 10.1109/TED.2003.811418.

[2]. T. Grasser, "Stochastic charge trapping in oxides: From random telegraph noise to bias temperature instabilities," *Microelectron. Rel.*, vol. 52, pp. 39-70, 2012, doi:10.1016/j.microrel.2011.09.002.

[3]. B. Kaczer, T. Grasser; Ph. J. Roussel; J. Franco; R. Degraeve; L.-A. Ragnarsson; E. Simoen, G. Groeseneken, H. Reisinger, "Origin of NBTI variability in deeply scaled pFETs," in *IEEE Proc. Int. Rel. Phys. Symp. (IRPS)*, May 2010, pp. 26–32, doi: 10.1109/IRPS.2010.5488856.

[4]. R. Wang, S. Guo, Z. Zhang, Q. Wang, D. Wu, J. Wang, R. Huang, "Too Noisy at the Bottom? -Random Telegraph Noise (RTN) in Advanced Logic Devices and Circuits," in *IEDM Tech. Dig.*, Dec. 2018, pp. 388–391, doi: 10.1109/IEDM.2018.8614594.

[5]. M. J. Kirton and M. J. Uren, "Noise in solid-state microstructures: A new perspective on individual defects, interface states and low-frequency (1/*f*) noise", *Advances in Physics*, vol. 38, no. 4, pp. 367-468, 1989, doi: 10.1080/00018738900101122.

[6]. A. J. Scholten, L.F. Tiemeijer, R. van Langevelde, R.J. Havens, A.T.A. Zegers-van Duijnhoven, V.C. Venezia, "Noise Modeling for RF CMOS Circuit Simulation", *IEEE Trans. Electron Devices*, vol. 50, no. 3, pp. 618–632, 2003, doi: 10.1109/TED.2003.810480.

[7]. M. Nour, Z. Celik-Butler, A. Sonnet, F.C. Hou, S. Tang, G. Mathur, "A stand-alone, physics-based, measurement-driven model and simulation tool for random telegraph signals originating from experimentally identified MOS gate-oxide defects," *IEEE Trans. Electron Devices*, vol. 63, no. 4, pp. 1428–1436, Apr. 2016, doi: 10.1109/TED.2016.2528218.

[8]. K. Sonoda, K. Ishikawa, T. Eimori, O. Tsuchiya, "Discrete Dopant Effects on Statistical Variation of Random Telegraph Signal Magnitude," *IEEE Trans. Electron Devices*, vol. 54, no. 8, pp.1981-1925, 2017, doi: 10.1109/TED.2007.900684.

[9]. K. Ito, T. Matsumoto, S. Nishizawa, H. Sunagawa, K. Kobayashi, H. Onodera, "Modeling of Random Telegraph Noise under Circuit Operation-Simulation and Measurement of RTN-induced delay fluctuation," in *Proc. 12th Int'l Symp. on Quality Electronic Design*, pp.22-27, 2011, doi: 10.1109/ISQED.2011.5770698.

[10]. M. Toledano-Luque, B. Kaczer, J. Franco, Ph.J. Roussel, T. Grasser, T.Y. Hoffmann, and G. Groeseneken, "From mean values to distributions of BTI lifetime of deeply scaled FETs through atomistic understanding of the degradation," in *Proc. Symp. Very Large Scale Integr. (VLSI) Technol.*, Jun. 2011, pp. 152–153.

[11]. M. Mehedi, K.H. Tok, J.F. Zhang, Z. Ji, Z. Ye, W. Zhang, J.S. Marsland, "An assessment of the statistical distribution of Random Telegraph Noise Time Constants," *IEEE Access*, vol. 8, no. 10, pp.1496-1499, 2020, doi: 10.1109/ACCESS.2020.3028747.

[12]. A.K.M.M. Islam and H. Onodera, "Worst-case Performance Analysis Under Random Telegraph Noise Induced Threshold Voltage Variability," in *Proc. 28th Int. Symp. Power and Timing Modeling, Optimization and Simulation (PATMOS)*, pp.140-146, 2018, doi: 10.1109/PATMOS.2018.8464147.

[13]. H. Miki, M. Yamaoka, N. Tega, Z. Ren, M. Kobayashi, C. P. D'Emic*, Y. Zhu, D. J. Frank, M. A. Guillorn, D.-G. Park, W. Haensch, and K. Torii, "Understanding Short-term BTI Behavior through Comprehensive Observation of Gate-voltage Dependence of RTN in Highly Scaled High-k / Metal-gate pFETs," in *Proc. Symp. Very Large Scale Integr. (VLSI) Technol.*, Jun. 2011, pp. 148–149.

[14]. J. F. Zhang, Z. Ji, W. Zhang, "As-grown-generation (AG) model of NBTI: A shift from fitting test data to prediction," *Microelectron. Rel.*, vol. 80, pp. 109-123, 2018, doi: /10.1016/j.microrel.2017.11.026.

[15]. H. Yang, M. Robitaille, X. Chen , H. Elgabra, L. Wei, and N.Y. Kim, "Random Telegraph Noise of a 28-nm Cryogenic MOSFET in the Coulomb Blockade Regime," *IEEE Electron Device Letters*, vol. 43, no. 1, pp.5-8, 2022, doi: 10.1109/LED.2021.3132964.

[16]. Y. Ye, C.-C. Wang, Y. Cao, "Simulation of Random Telegraph Noise with 2-Stage Equivalent Circuit," in *IEEE/ACM Int. Conf. on Computer-Aided Design (ICCAD)*, San Jose, CA, 2010, pp. 709-713.

[17]. P. Weckx, M. Simicic, K. Nomoto, M. Ono, B. Parvais, B. Kaczer, P. Raghavan, D. Linten, K. Sawada, H. Ammo, S. Yamakawa, A Spessot, D. Verkest, A. Mocuta, "Defect-based compact modeling for RTN and BTI variability," in *Proc. Int. Rel. Phys. Symp.*, 2017, pp. CR-7.1-CR-7.6.

[18]. R. Gao, M. Mehedi, H. Chen, X. Wang, J.F. Zhang, X.L. Lin, Z.Y. He, Y.Q. Chen, D.Y. Lei, Y. Huang, Y.F. En, Z. Ji, and R. Wang, "A fast and test-proven methodology of assessing RTN/fluctuation on deeply scaled nano pMOSFETs," in *Proc. Int. Rel. Phys. Symp.*, 2020.

[19]. M. Mehedi, K.H. Tok, Z. Ye, J.F. Zhang, Z. Ji, W. Zhang, J.S. Marsland, "On the accuracy in modelling the statistical distribution of Random Telegraph Noise Amplitude," *IEEE Access*, vol. 9, pp.43551-43561, 2021, doi: 10.1109/ACCESS.2021.3065869.

[20]. T. Nagumo, K. Takeuchi, T. Hase, and Y. Hayashi, "Statistical Characterization of Trap Position, Energy, Amplitude and Time Constants by RTN Measurement of Multiple Individual Traps," in *IEDM Tech. Dig.*, Dec. 2010, pp. 628–631, doi: 10.1109/IEDM.2010.5703437.

[21]. M. Tanizawa, S. Ohbayashi, T. Okagaki, K. Sonoda, K. Eikyu, Y. Hirano, K. Ishikawa, O. Tsuchiya, and Y. Inoue, "Application of a Statistical Compact Model for Random Telegraph Noise to Scaled-SRAM Vmin Analysis," in *Proc. Symp. VLSI Technol.*, Jun. 2010, pp. 95–96, doi: 10.1109/VLSIT.2010.5556184.

[22]. M. Duan, J. F. Zhang, Z. Ji, W. Zhang, B. Kaczer, T. Schram, R. Ritzenthaler, A. Thean, G. Groeseneken, and A. Asenov, "Time-dependent variation: A new defect-based prediction methodology," in *Proc. Symp. Very Large Scale Integr. (VLSI) Technol.*, Jun. 2014, pp. 74–75.

[23]. A. Manut, R. Gao , J.F. Zhang , Z. Ji , M. Mehedi, W. Zhang, D. Vigar, A. Asenov, and B. Kaczer, "Trigger-When-Charged: A Technique for Directly Measuring RTN and BTI-Induced Threshold Voltage Fluctuation Under Use-Vdd," *IEEE Trans. Electron Devices*, vol. 66, no.3, pp. 1482-1488, 2019, doi: 10.1109/TED.2019.2895700.

[24]. P. Saraza-Canflanca, J. Martin-Martinez, R. Castro-Lopez, E. Roca, R. Rodriguez, F.V. Fernandez, and M. Nafria, "Statistical Characterization of Time-Dependent Variability Defects Using the Maximum Current Fluctuation," *IEEE Trans. Electron Devices*, vol. 68, no.8, pp. 4039-4044, 2021, doi: 10.1109/TED.2021.3086448.

[25]. M. Duan, J.F. Zhang, Z. Ji, W. Zhang, B. Kaczer, T. Schram, R. Ritzenthaler, G. Groeseneken, and A. Asenov, "New analysis method for time-dependent device-to-device variation accounting for within-device fluctuation," *IEEE Trans. Electron Devices*, vol. 60, no. 8, pp. 2505–2511, Aug. 2013, doi: 10.1109/TED.2013.2270893.

[26]. J. F. Zhang, S. Taylor, and W. Eccleston, "Electron trap generation in thermally grown SiO_2 under Fowler-Nordheim stress," *J. Appl. Phys.*, vol. 71, pp. 725-734, 1992, doi: 10.1063/1.351334.

[27]. T. Grasser, K. Rott, H. Reisinger, M. Waltl, P. Wagner, F. Schanovsky, W. Goes, G. Pobegen, and B. Kaczer, "Hydrogen-Related Volatile Defects as the Possible Cause for the Recoverable Component of NBTI," in *IEDM Tech. Dig.*, Dec. 2013, pp. 409–412, doi: 10.1109/IEDM.2013.6724637.

[28]. R. Gao, A. B. Manut, Z. Ji, J. Ma, M. Duan, J. F. Zhang, J. Franco, S. W. M. Hatta, W. Zhang, B. Kaczer, D. Vigar, D. Linten, and G. Groeseneken, "Reliable time exponents for long term prediction of negative bias temperature instability by extrapolation," *IEEE Trans. Elec. Dev.*, Vol. 64, pp. 1467-1473, 2017, doi: 10.1109/TED.2017.2669644.